AFRL-RV-PS-
TR-2015-0150
AFRL-RV-PS-
TR-2015-0150

SURFACE WAVE ATTENUATION IN THE TIBETAN PLATEAU FROM AMBIENT NOISE

Xiaodong Song, et al.

University of Illinois at Urbana-Champaign
Department of Geology
605 E. Springfield Ave.
Champaign, IL 61820

31 August 2015

Final Report

APPROVED FOR PUBLIC RELEASE; DISTRIBUTION IS UNLIMITED.

AIR FORCE RESEARCH LABORATORY
Space Vehicles Directorate
3550 Aberdeen Ave SE
AIR FORCE MATERIEL COMMAND
KIRTLAND AIR FORCE BASE, NM 87117-5776

DTIC COPY

NOTICE AND SIGNATURE PAGE

Using Government drawings, specifications, or other data included in this document for any purpose other than Government procurement does not in any way obligate the U.S. Government. The fact that the Government formulated or supplied the drawings, specifications, or other data does not license the holder or any other person or corporation; or convey any rights or permission to manufacture, use, or sell any patented invention that may relate to them.

This report was cleared for public release by the 377 ABW Public Affairs Office and is available to the general public, including foreign nationals. Copies may be obtained from the Defense Technical Information Center (DTIC) (http://www.dtic.mil).

AFRL-RV-PS-TR-2015-0150 HAS BEEN REVIEWED AND IS APPROVED FOR PUBLICATION IN ACCORDANCE WITH ASSIGNED DISTRIBUTION STATEMENT.

//SIGNED//	//SIGNED//
Dr. Robert Raistrick	Glenn M. Vaughan, Colonel, USAF
Project Manager, AFRL/RVBYE	Chief, Battlespace Environment Division

This report is published in the interest of scientific and technical information exchange, and its publication does not constitute the Government's approval or disapproval of its ideas or findings.

REPORT DOCUMENTATION PAGE

Form Approved
OMB No. 0704-0188

1. REPORT DATE *(DD-MM-YYYY)*	**2. REPORT TYPE**	**3. DATES COVERED** *(From - To)*
31-08-2015	Final Report	01 May 2012 to 31 Aug 2015

4. TITLE AND SUBTITLE
Surface Wave Attenuation in the Tibetan Plateau from Ambient Noise

5a. CONTRACT NUMBER
FA9453-12-C-0209

5b. GRANT NUMBER

5c. PROGRAM ELEMENT NUMBER
62601F

6. AUTHOR(S)
Xiaodong Song, Richard Weaver, and Xiaoning (David) Yang[1]

5d. PROJECT NUMBER
1010

5e. TASK NUMBER
PPM00013633

5f. WORK UNIT NUMBER
EF007745

7. PERFORMING ORGANIZATION NAME(S) AND ADDRESS(ES)
University of Illinois at Urbana-Champaign
Department of Geology
605 E. Springfield Ave.
Champaign, IL 61820

[1]Los Alamos National Laboratory
PO Box 1663
Los Alamos, NM 87545

8. PERFORMING ORGANIZATION REPORT NUMBER

9. SPONSORING / MONITORING AGENCY NAME(S) AND ADDRESS(ES)
Air Force Research Laboratory
Space Vehicles Directorate
3550 Aberdeen Avenue SE
Kirtland AFB, NM 87117-5776

10. SPONSOR/MONITOR'S ACRONYM(S)
AFRL/RVBYE

11. SPONSOR/MONITOR'S REPORT NUMBER(S)
AFRL-RV-PS-TR-2015-0150

12. DISTRIBUTION / AVAILABILITY STATEMENT
Approved for public release; distribution is unlimited. (377ABW-2015-0789 dtd 07 Oct 2015)

13. SUPPLEMENTARY NOTES

14. ABSTRACT
We explore the methodologies to extract amplitude information from the empirical Green functions (EGF) derived from ambient noise correlations and to map the attenuation of the surface waves. Our approaches are to combine theoretical derivations, numerical simulations, and practical considerations. Theoretical insights show that even in the case of incompletely diffuse noise fields, we can robustly recover not only travel times, but also ray arrival amplitudes and attenuation. We investigate two approaches with detailed formulations: linear array methods and more general methods for 2D station networks. Our numerical simulations validate that amplitudes and attenuations can indeed be extracted from noise correlations for a linear array or for a more general 2D array. We developed a temporal flattening procedure, which is effective in speeding up convergence while preserving relative amplitudes. For real data, we developed an "asynchronous" temporal flattening procedure that does not require all stations to have data at the same time. Tests on real data suggest attenuations extracted from our noise-based methods are comparable with those from earthquakes. A preliminary attenuation map of Chinese continent is obtained based on earthquake data. Internal scattering can be important in contaminating the amplitude of the main arrivals, which need to be considered when making amplitude measurements. Our studies show the great promise of retrieving amplitude and attenuation information from ambient noise correlations and suggest practical methods for applications to real data.

15. SUBJECT TERMS
attenuation, surface waves, noise correlations

16. SECURITY CLASSIFICATION OF:			**17. LIMITATION OF ABSTRACT**	**18. NUMBER OF PAGES**	**19a. NAME OF RESPONSIBLE PERSON**
a. REPORT	**b. ABSTRACT**	**c. THIS PAGE**			Dr. Robert Raistrick
Unclassified	Unclassified	Unclassified	Unlimited	22	**19b. TELEPHONE NUMBER** *(include area code)*

This page is intentionally left blank.

Table of Contents

List of Figures

1. Summary

In this project, we explore the methodologies to extract amplitude information from the empirical Green functions (EGF) derived from ambient noise correlations and to map the attenuation of the surface waves. Our objectives are: (1) To develop methods for extracting attenuation from ambient noise; (2) To develop methods for practical applications using the Tibetan Plateau as a test bed; (3) To develop preliminary surface wave attenuation maps of the Tibetan Plateau. Our approaches are to combine theoretical derivations, numerical simulations, and practical considerations. A particular problem in retrieving amplitudes from noise is that seismic ambient noise source is not uniform and it changes with time. Overall, our studies show great promise for retrieving amplitude and attenuation information from ambient noise correlations and suggest practical methods for applications to real data.

Theoretical insights show that even in the case of incompletely diffuse noise fields, we can robustly recover not only travel times, but also ray arrival amplitudes and attenuation. We investigated two approaches with detailed formulations: linear array methods and more general methods for 2D station networks. Our numerical simulations validate that amplitudes and attenuations can indeed be extracted from noise correlations for a linear array or for a more general 2D array. We developed a temporal flattening procedure, which is effective in speeding up convergence while preserving relative amplitudes. For real data, we developed an “asynchronous” temporal flattening procedure that does not require all stations to have data at the same time. Tests on real data suggest attenuations extracted from our noise-based methods are comparable with those from earthquakes. A preliminary attenuation map of China is obtained based on earthquake data. Internal scattering can be important in contaminating the amplitude of the main arrivals, which need to be considered when making amplitude measurements.

2. Introduction

The objectives of this research are to develop methods for extracting attenuation from ambient noise, to develop methods for practical applications using the Tibetan Plateau as a test bed, and to develop preliminary surface wave attenuation maps of the Tibetan Plateau.

A particular problem in retrieving amplitudes from noise is that the seismic ambient noise source is not uniform and it changes with time. Our approaches are to combine theoretical derivations, numerical simulations, and practical considerations. This report summarizes the results that we have made on all the fronts outlined in the initial proposal, including the basic theoretical approaches, results using numerical simulations, practical considerations with real data, and a preliminary attenuation map of Chinese continent. We also address a key issue on amplitude measurements in the presence of internal

scattering using numerical simulations, which could be important for the real Earth. Overall, our studies show the great promise of retrieving amplitude and attenuation information from ambient noise correlations and suggest practical methods for applications to real data.

3. Technical Approaches

3.1. Theoretical formulations for extracting attenuation from ambient noise

Weaver (2011) provides a theoretical derivation that, even in the case of an incompletely diffuse noise field, permits cross-correlation to robustly recover not just travel times, but also ray arrival amplitudes, the ambient field's specific intensity, the strength and density of its scatterers if any, and most importantly attenuation. A full examination of the amplitude X of a correlation waveform between stations *i* and *j* shows that it takes the form

$$X_{ij} = 2 s_i s_j B_i(\hat{n}_{i\to j}) \sqrt{2\pi c / (\omega_o |x_i - x_j|)}\, \exp(-\alpha |x_i - x_j|) \qquad (1)$$

where a is the average attenuation between stations *i* and*j*; ω_o is the frequency; c is wavespeed, and s_i and s_j are site effects at the two stations.

B_i is the ambient intensity in the direction from *i* towards *j* evaluated at station *i*. An important and useful result for this research is that the ray amplitude *X* depends only on *B* in that direction as an asymptotically valid approximation (at the next order, the differences with respect to direction are on the order 1% or less).

3.2 In the case of a linear array

For a linear array, along a direction $\hat{n}$ of several seismic stations, the amplitudes X_{ij} of cross correlation arrivals for j > i should be

$$X_{i<j} = 2 s_i s_j B_i(\hat{n}_{i\to j}) \sqrt{2\pi c / (\omega_o |x_i - x_j|)}\, \exp\left(-\int_{x_i}^{x_j} \alpha\, dx\right). \qquad (2)$$

Formulation I-1: path average. Eqn (2) indicates that amplitude X from station i (near one end of the array) to all stations j in one direction (to the other end of the array) depends only on the intensity at station i along the same strike direction. Thus the slope of the logarithm of the geometrically corrected amplitude, X*sqrt(distance), as a function of distance would give an estimate of the average attenuation (coefficient **a**) along the linear array.

Formulation I-2: inversion for a linear array. The system in eqn (2) can be linearized by taking the logarithm as in traditional earthquake-based attenuation studies (e.g. Yang et al., 2004). This system is overdetermined and can be solved with a reasonable number

of stations. Taking N to be the number of stations along this array, we have at most N(N-1)/2 such ray-amplitudes in one direction. Using one parameter per station to describe the local attenuation, there are up to 3N unknowns (the site factor, the B value along direction $\hat{\boldsymbol{n}}$, and using one local attenuation factor at each station). Correlations from the direction $-\hat{\boldsymbol{n}}$ can provide up to N(N-1)/2 additional amplitudes and N additional unknowns B. Thus if amplitudes along both directions are available, one needs only 5 to 7 stations along this line to solve all unknowns. This is a very general approach without *a priori* constraints on the noise intensity.

Formulation I-3: assuming no internal scattering. The noise intensity cannot be arbitrary. If we assume the ambient noise sources are from the far field (the oceans as many studies have pointed out for the seismic bands we are interested in) and further assume that scattering is not important, it can be shown that the noise intensity B decays like exp(-2*a*distance), where a is the same medium attenuation coefficient we try to extract. Thus in this formulation, we need only two Bs (one at either end of the linear array).

3.3 The case of a 2D station network

Formulation II. In general, we have a network of stations whose distribution is irregular throughout the study region. However, we may often be able to identify 3 or more stations that roughly lie on the same great circle path. In this case, we can use amplitude ratios to eliminate the unknown intensity B along that direction. Similar ideas are commonly used in earthquake studies to measure phase velocity between two stations (the "two-station" method) or derive surface attenuation using amplitude ratios between two stations along the great circle with the earthquake (e.g. Yang et al., 2004).

Consider 3 stations (station 1, 2, 3) on the same great circle, the ratios of the *geometrically-corrected* amplitudes $X_{13}/X_{12}=s_3/s_2 \exp(-a_2x_2)$, $X_{31}/X_{32}= s_1/s_2 \exp(-a_1x_1)$, where s_i is the site factor for station i, x_1 and x_2 are distance between stations 1 and 2 and stations 2 and 3, respectively, and a_1 and a_2 are average attenuation coefficients between stations 1 and 2 and stations 2 and 3. If we assume no internal scattering, such that intensity B decays like exp(-2a*distance) as discussed above, we can use two other amplitude ratios: $X_{23}/X_{12}=s_3/s_1 \exp(-a_1x_1-a_2x_2)$, and $X_{21}/X_{32}=s_1/s_3 \exp(-a_1x_1-a_2x_2)$. The logarithm of such an amplitude ratio is linear to distance. Once enough amplitude ratios are measured along paths of different azimuths and locations to provide sufficient coverage, it is straightforward to discretize the region and construct a tomographic inversion for the attenuation coefficients for the entire region.

4. Results

4.1. Numerical simulations: Tests on linear arrays

We show a numerical simulation to demonstrate that attenuation can be extracted along a linear array using simulated data with an azimuthally varying noise source (**Fig. 1**). The simulations included a simple case of a uniformly spaced linear array of receivers, homogeneous attenuation and wave speed and mild directionality to the noise field. The temporal asymmetry in **Fig. 1B** indicates that the on-strike noise intensities in the two directions are not equal. Note that amplitude decay is evident at positive lapse time (in direction from left to right, i.e., 6->5, …, 6->1 in **Fig. 1A**) due to geometric and intrinsic attenuation. However, the amplitudes at the negative lapse time in the EGF are nearly constant. This is the result of a complex product of geometric and exponential attenuation and the differences between the noise intensities B at the different stations, consistent with the theory. The rays at the negative lapse time are 5->6, …, 1->6 (originated at different stations). Theorefore, the amplitudes are B_i (going rightward) * exp(-α*distance) / sqrt(distance), where i is 5, 4, 3, 2 or 1 respectively, so B_i decays as exp (+ 2 α*distance). The net effect is exp(+ α* distance) / sqrt(distance), which is roughly constant from our model inputs.

The simulation shows that accurate attenuations and site factors can be accurately retrieved (**Fig. 2**; Weaver, 2011). Furthermore, errors in attenuation measurements can also be determined (**Fig. 2**; Weaver, 2013).

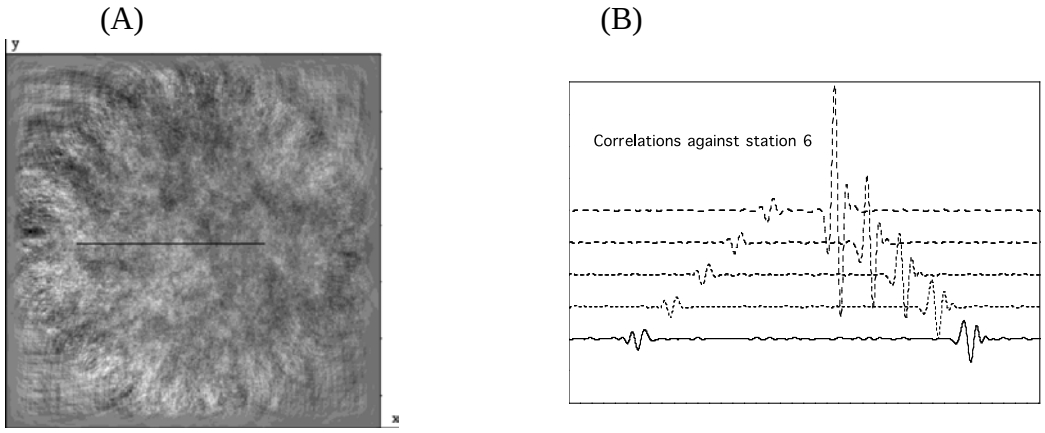

Fig. 1. (**A**) Simulation 'A'. Snapshot of the broad-band wavefield in a 271 × 271 array, which seismically scales to 800 km, before bandpass filtering. *The strong absorption on the edges and anisotropic annulus of sources are evident. The horizontal line indicates the line along which six stations were uniformly placed in the simulation.* (**B**) Stack of correlation waveforms between station 6 (the rightmost in **A)** and the five others (from top to bottom are 6-5, …, 6-1, respectively).

(A) (B)

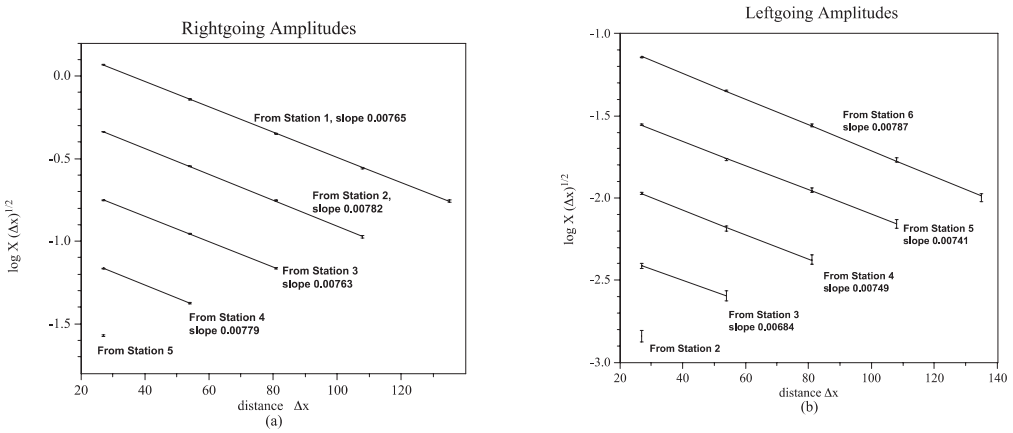

Fig. 2. (**A**) The amplitudes X of the arrival wave packets in the right-going correlation waveforms from simulation 'A' are plotted versus interstation distance. *One-sigma error bars are for δlogX = δX/X (from Table 1 of Weaver, 2013). Amplitudes corresponding to the same pseudo-source fit well to straight lines. The observed slopes correspond well to the expected 0.00777 nepers per mesh spacing.* (**B**) The left-going amplitudes in the simulation 'A' have larger error bars, corresponding to the relatively weaker ambient noise intensity coming from the right.

4.2 Numerical simulations: "Earth-like" temporally variable noise field

1) A 1D array case

To examine our ability to extract attenuation from ambient noise methods, we impose Earth-like temporally variable noise intensity on a simulated diffuse field. The setup for our simulation is shown in **Fig. 3**. The source intensity includes smoothly varying as well as a strong "local" intensity (as indicated from the shade on the source "ring"). The study region is divided into four parts, inside the source "ring". 10 receiver stations with spacing distance of 85 km were arranged in a linear array, where 5 receiver stations are in the lower left region and the other 5 receiver stations are located in the upper right region. An attenuation model with two different attenuation coefficients, $\alpha_1 = 0.00259$ in the lower left region and $\alpha_2 = 0.00388$ in the upper right region, was configured. The site responses of all stations in the experiment are set to 1.

We add the seismic data from a station in USArray into our simulation data to simulate the natural seismic noise. The seismic noise is from a 4-year continuous seismic waveform after clipping earthquakes and spikes. We then multiply this seismic noise with the synthetic noise field point by point to generate the synthetic noise field with temporally varying strength. We refer to the original simulation data as "original" data and the data with seismic noise as "raw" data, in our discussion below. The sample rate of the data is 3 points per second, and a total of about 1 year of data are generated at each station.

In order to retain rapid convergence amidst time-varying noise intensity, we developed a "temporal flattening" procedure (Weaver, 2011; Song et al. 2012). Every station's band-limited signal is normalized by a running average of the *total* band-limited array energy. Thus each station is treated equally, and relative amplitudes are preserved.

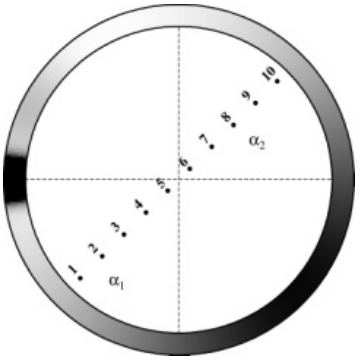

Fig. 3. Simulation 'B'. Distribution of source intensity and receiver locations. *The Gaussian noise source is highly non-uniform as indicated by the shades along the circumference. We have also added temporal variation of the noise source, which mimics temporal variation of a seismic station on Earth. The attenuation inputs include four different values at the four quadrants.*

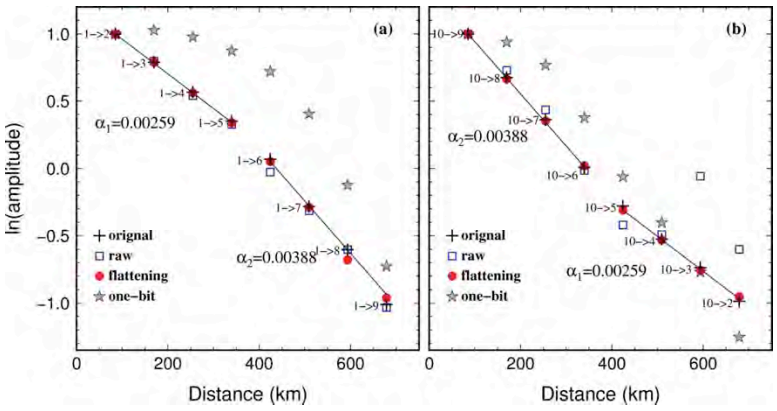

Fig. 4. Amplitudes extracted from GFs with different pre-processing procedures for Simulation 'B'. *The lines are true values from the inputs.* (**A**) from Station 1 to other stations. (**B**) from Station 10 to other stations.

We see that the amplitude decays of the "raw" data are similar to that of the "original". But when the signal to noise ratios of the GFs are low (e.g., **Fig. 4B, right side**), the amplitudes are not stable. The amplitudes from the one-bit processing are apparently not correct; the behavior is not linear. The amplitude decays from the flattening procedure are very close to the true values.

2) A 2D array case

The set up for this simulation (Simulation 'C') is the same as above, but the wavefield is recorded at a 2D array (10x10 or a total of 100 stations with uniform spacing). The input attenuation of the medium is not uniform: it has four different values at the four quadrants of the array. Following Formulation II-1, we identify linear arrays within an azimuth of 10 degrees for each station. We then form amplitude ratios for stations along each linear array. We obtain a total of about 5600 independent amplitude ratios. These amplitude ratios are then used to invert for 2D attenuation maps and site factors. The inversion with 4 cells (as in the input model) recovers perfectly the input model and the inversion with 36 cells recovers quite well the input model except cells at the corner which are not constrained by the amplitude ratios (**Fig. 5**).

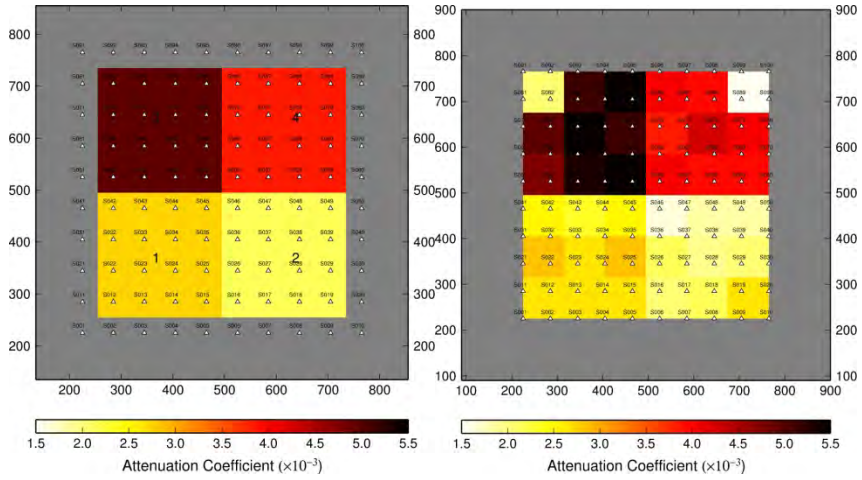

Fig. 5. Extraction of attenuation from 2D array with simulated data (Simulation 'C'). *The input model has four different values at the four quadrants, respectively. The noise source varies in strength azimuthally.* (**A**) The input Qs are fully recovered using a 4-cell parameterization. (**B**) The input Qs are reasonably recovered in a 36-cell inversion, except at the four corners, which are not constrained by the method.

4.3. Tests on real data

We have conducted various tests on amplitude extractions from real data. Here we show some test results using stations in the western U.S. (**Fig. 6**). We have dealt with a number of practical issues, including the issue of energetic arrivals and that the fact not all stations have signals and energetic arrivals may appear at different times for different stations (**Fig. 7**), a new "asynchronous" temporal flattening (ATF) procedure (**Fig. 8**), and the issue of window length for the flattening procedure (**Fig. 9**). The amplitude attenuations extracted from the ambient noise seem compatible with those from earthquakes (**Fig. 10**).

Because not all stations have signals and energetic arrivals may appear at different times for different stations, if we require all stations have exactly the same overlapping time segments, we will throw away lots of data, making the convergence of GFs difficult. To address this issue, we developed a new "asynchronous" temporal flattening (ATF) procedure, as follows.

1) Window out energetic signals for each individual trace. Keep track of points that are kept and points that are windowed out.
2) Select a window length for ATF.
3) Calculus RMS amplitude of ALL traces for that time window. Only points that have been kept after windowing are used.
4) Divide each trace within the time window by the RMS.

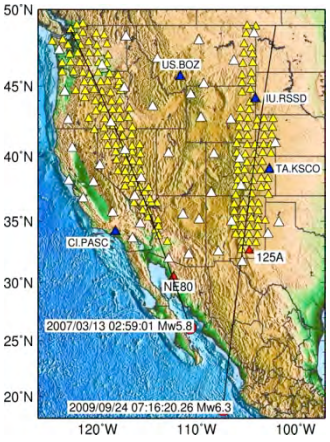

Fig. 6. Map of stations in the western U.S. used in our tests. *Indicated also are two earthquakes used to compare with ambient noise results.*

Fig. 7. Data preprocessing. *For a given trace, energetic signals are first windowed out. A flag trace is constructed to keep track of points that are kept (values of 1) or windowed out (values of 0). The windowed trace is then "flattened" using the average root-mean-square amplitude over a period of time (e.g. hours) using all stations and data points that have not been windowed out.*

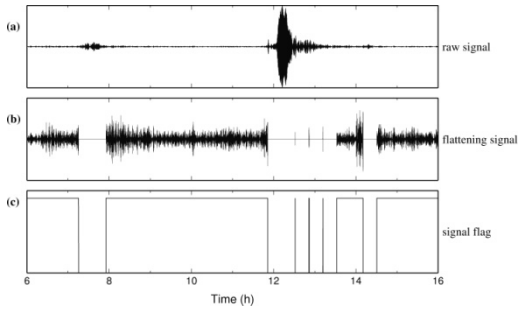

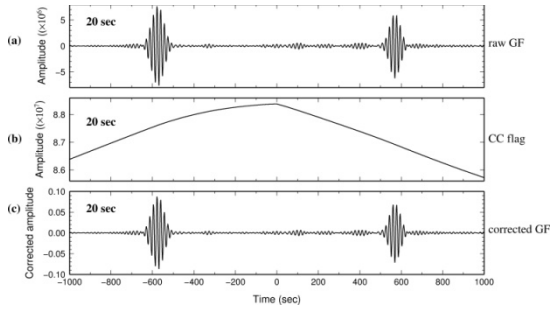

Fig. 8. (**A**) A raw empirical Greens function (EGF) is constructed from the cross-correlation of "flattened" traces. (**B**) Cross-correlation is constructed using the flag traces, which indicates the number of data points that have been used in the EGF for a given time lapse. (**C**) The raw EGF is normalized by the number of data points in the flag CC to yield the normalized EGF.

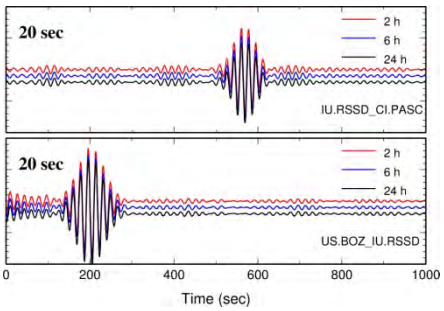

Fig. 9. Tests on the windows used in the temporal flattening procedure. *Shown are results for window length of 2 hours to 24 hours. The traces and amplitudes are identical and thus our window length in the flattening procedure can be quite wide (1 day).*

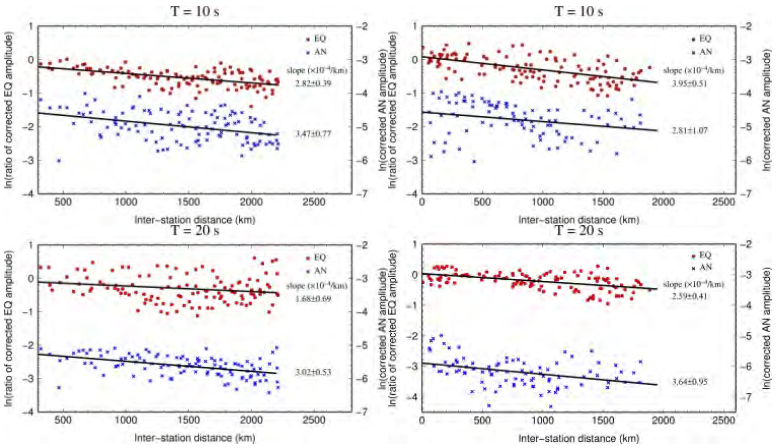

Fig. 10. Comparison of amplitude decays obtained from earthquakes (red dots) and ambient noise (blue crosses) at two periods (10 and 20 s). *Left two panels are for the western group of stations and the event in 2007 (**Fig. 4**) and right panels are for the eastern group of stations and the event in 2009. Approximately 18 months of ambient noise data are used in calculating the EGFs.*

4.4 Tests using correlation of the coda of noise correlation (C^3)

We tested a methodology to construct accurate empirical Green functions (EGFs), including the correct amplitude, from noise cross-correlation (*NCC*) (Zhang and Yang, 2013). The method is based on the correlation of coda of noise correlation (C^3). Stehly *et al.* (2008) first proposed the method to improve the signal-to-noise ratio (SNR) and time symmetry of EGF. We found that the method is also effective in reducing the effect of uneven noise-source distribution on EGF amplitudes and the resulting attenuation-estimate bias, particularly for long-period data (18 s).

Fig. 11 gives some linear array examples illustrating the effectiveness of the C^3 method. We use USArray Transportable Array (TA) stations in the examples. We first select station MLAC as the end station of six linear arrays in different directions and a colocated earthquake (2007/6/12, Mw 4.6). We then calculate C^3 for these linear arrays using additional stations, as required by the C^3 method, along the coast. We also calculate direct *NCC* for the arrays and measure earthquake-signal amplitudes for comparison. Before calculating C^3, transient-removed noise data are preprocessed with temporal flattening. For direct *NCC*, noise data are preprocessed with running-absolute-mean (RAM) normalization (without temporal flattening) (Bensen, *et al*., 2007). We measure amplitudes from EGFs that represent outgoing energy from the end station (positive-lag EGF). All amplitudes are from data filtered around 18 s.

For 4 of the 6 lines in Figure 11 (Lines 3, 4, 5 and 6), C^3-derived EGFs yield attenuation estimates that are fairly consistent with those from the earthquake, whereas except for Line 4, estimates from *NCC*-derived EGFs are much lower or even negative. For Line 1, because the positive-lag EGFs from *NCC* have very poor SNR, we are not able to make a *NCC*-based estimate. Nevertheless, C^3-based attenuation estimate for Line 1 is less consistent with the earthquake estimate compared with the 4 better lines. One of the possible reasons for the inconsistency is that there are only 5 stations for the line and C^3 EGF amplitudes show large variations. These factors certainly reduce the reliability of the estimate, which has an uncertainty of ±22e-4, the largest among all lines in Figure 1. Line 2 is another example showing noise attenuation estimates that are different from the earthquake estimate. For this line, earthquake amplitudes increase significantly with increasing distance, yielding an apparent attenuation coefficient of -4.9e-4, whereas noise EGF amplitudes decrease. Although it requires more detailed analysis to adequately explain this observation, there are several factors that could potentially contribute to the observed discrepancy. These factors include the difference between an earthquake and the virtual source at the end station in terms of source size, mechanism and location including depth, and possible different path and/or site responses to earthquake and noise signals. These factors may also explain the observation that amplitude variations among stations in a line array sometimes exhibit different behavior between noise EGFs and earthquake signals.

Our examples show that the attenuation coefficients from C^3-derived EGF correlate well with those from earthquakes, suggesting that C^3 processing is promising in extracting surface-wave attenuation from noise. However, direct NCC with only the RAM normalization in preprocessing is problematic in extracting attenuation in real data.

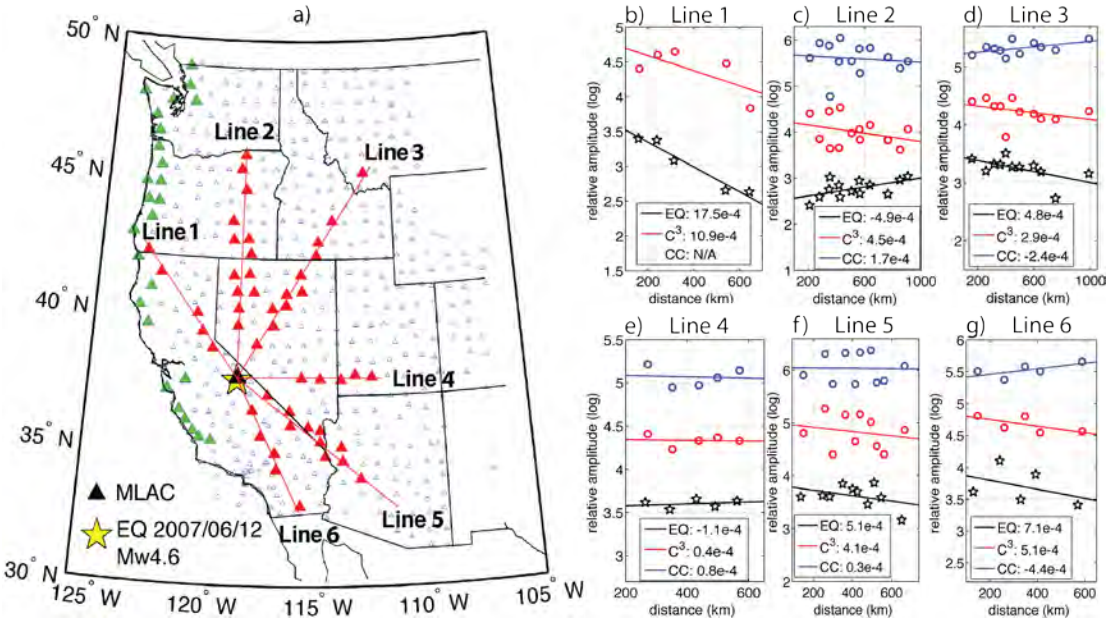

Fig. 11. Comparison of attenuation coefficients extracted from C^3 and *NCC* of 18-s noise with that from an earthquake for six linear arrays sampling different directions. *(**a**) Map of the western U.S. showing USArray TA stations (blue triangles), an earthquake (yellow star, 2007/06/12 Mw4.6 37.54N 118.86W), the six linear arrays (red triangles), the end station MLAC (black triangle) and additional stations used for C^3 calculations (green triangles). (**b**–**g**) Comparison of the apparent attenuation estimated from the geometric-spreading corrected earthquake amplitudes (black) with those estimated from C^3 (red) and NCC-derived (blue) EGF. (NCC fails for Line 1 due to poor SNR.) Straight lines are the best fits to the log amplitudes. Estimated attenuation coefficients are listed in the insets.*

4.5 Influence of internal scattering

For practical applications to the real Earth, complexity of the Earth's media has to be considered. The complexity includes 3D-velocity structure, which can cause focusing and

defocusing effect, as well as scattering. Amplitude measurements in real data typically have large scatters, whether they are based on noise correlations or earthquake data (see above). In an effort to understand influences of these factors, we investigated the influence of internal scattering with numerical simulation (**Fig. 12**). In this case, the waveforms of the EGFs become more complicated with scattered energy arriving before and after the main arrival (**Fig. 12B**), compared with the case without internal scattering (e.g. **Fig. 1, Right**). The attenuation (intrinsic attenuation plus scattering) can still be extracted (**Fig. 12C**), which suggest that scattering and intrinsic attenuation both contribute to the decay of amplitudes and from the decay alone, intrinsic attenuation and scattering cannot be distinguished. Furthermore, the recovery of the amplitude "attenuation" has greater uncertainties because of more complex waveforms. This may explain variations of amplitude and attenuation measurements in real data. Exploration of internal scattering and intrinsic attenuation may help us understand their effect on amplitudes and design strategies for more stable amplitude measurements.

The results of our investigations on internal scattering can be summarized as follows. Internal scattering can be important in contaminating the amplitude of the main arrivals. (1) The different sources of attenuation are additive, as expected. If we only examine at the level of analysis in which we simply plot log A vs. distance, there is no way to distinguish. (2) The arrival wave packets are much less well resolved - assessment of amplitude A is more problematic and in consequence the fits of log A vs. distance are less clean (with larger errors). The reasons include: a) Coda and the related pulse broadening contaminates the waveform at times at and after the main arrival and b) Spurious arrivals (due to a combination of scattering and incomplete diffuseness) contaminate the waveform at times at and before the main arrival.

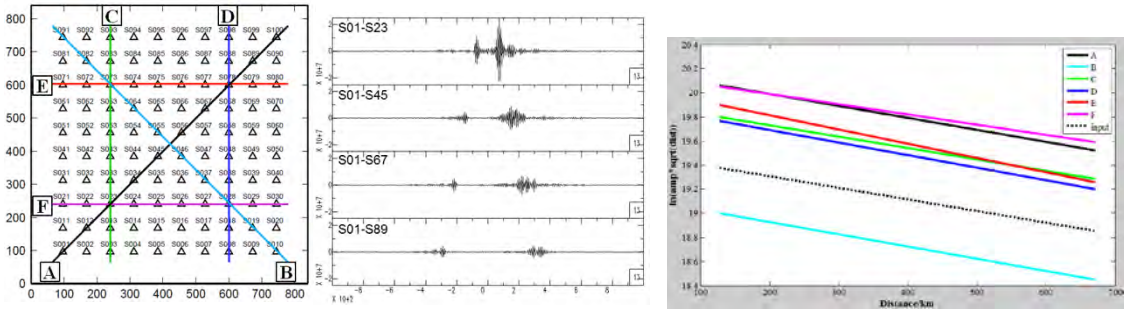

Fig. 12. Tests with simulated data with internal scattering. *The attenuation due to scattering is half of the attenuation due to intrinsic absorption, and together gives a total attenuation coefficient of about 0.000965. (**A**) Station distribution and 6 example arrays. (**B**) The EGFs obtained from inter-station correlations along the diagonal array A. The codas seem quite strong, and even become comparable with the main arrival at larger distances, which make the amplitude difficult to measure. (**C**) Decay of amplitude with distance for the 6 example arrays (lines A through F in **Fig. 11A**). Here the amplitude is defined by the difference between the maximum and the minimum amplitude in the EGFs. Although the measurements seem to be more varied than without scattering, the slopes generally agree with the input (dotted line).*

4.6 A preliminary attenuation model of China (including the Tibetan Plateau)

We have shown above that amplitude measurements from noised-based measurements and earthquake-based measures are compatible for similar paths from limited studies. We eventually would like to develop an attenuation model with increased coverage based on both earthquake and noise-based data. We have performed Rayleigh wave attenuation tomography in the Chinese mainland at the period of 20 s using earthquake data. We use over 200 earthquakes recorded by some 800 stations of CRSN (**Fig. 13**, Left). We adapted a phase matching technique to semi-automatic processing, which allowed us to obtain a large quantity of high-quality Rayleigh wave amplitude measurements. After initial data processing, which includes grouping and clustering stations to generate station pairs of similar azimuths, calculating the amplitude ratios in each group, and rejecting data with large residuals, we extracted more than 60000 paths of amplitude ratios. **Fig. 12** (right) shows the attenuation map for 20 s Rayleigh wave. The image reveals low attenuation in the main basins and the stable blocks and high attenuation in the orogens in the Western China.

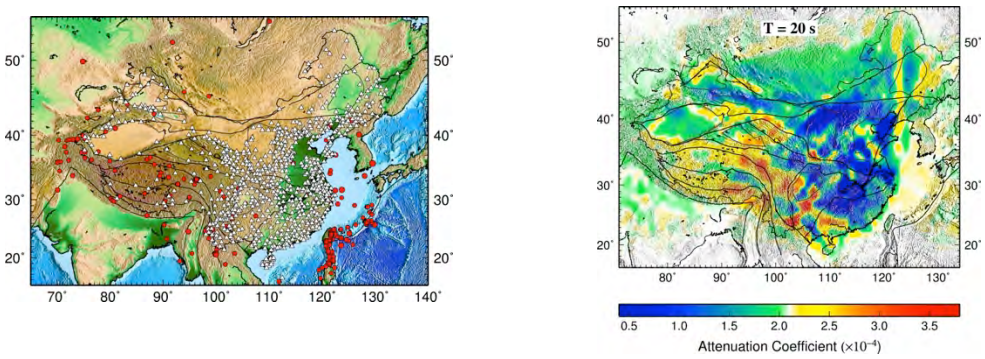

Fig. 13. A preliminary Rayleigh wave attenuation study of China using earthquake data. ***(Left)*** *Distributions of earthquakes (red dots) and stations (white triangles) used. The events are Mw 4.8 or greater over a period of 1.5 years (Jan. 2010 to June 2011).* ***(Right)*** *Rayleigh wave attenuation map at 20 s based on earthquake data.*

5. Conclusions

The specific findings are listed below. Our studies show the great promise of retrieving amplitude and attenuation information from ambient noise correlations and suggest practical methods for applications to real data. We also examined amplitude measurements in the presence of internal scattering. The studies set the stage for applying the new methods to mapping attenuation structure.

1) Theoretical derivations suggested that noise correlations are proportional to Green's functions, even in the presence of non-uniform and anisotropic source.
2) We formulated and tested several approaches using numerical simulations for both linear arrays and 2D arrays. The results show near perfect agreement (including error estimates) in extracted attenuation between theory and simulations.
3) We developed a temporal flattening procedure that is effective in speeding up convergence while preserving relative amplitudes. For real data, we developed an "asynchronous" temporal flattening procedure that does not require all stations to have data at the same time. The flattening procedure can have a long window length (1 day).
4) Limited tests on real data suggest estimated attenuation values are comparable to those from earthquakes.
5) Tests using C^3 processing show that attenuation coefficients from C^3-derived EGFs correlate well with those from earthquakes, suggesting that the C^3 processing is also promising. Simple CC preprocessing procedures, such as running-average-mean or one-bit, cannot produce correct attenuation values and should be avoided.
6) We developed a preliminary attenuation model of China (including the Tibetan Plateau) using the earthquake-based data.
7) Internal scattering can be important in contaminating the amplitude of the main arrivals, which needs to be considered when making amplitude measurements.

REFERENCES

Bensen, G. D., M. H. Ritzwoller, M. P. Barmin, A. L. Levshin, F. Lin, M. P. Moschetti, N. M. Shapiro, and Y. Yang, Processing seismic ambient noise data to obtain reliable broad-band surface wave dispersion measurements, *Geophys. J. Int.*, *169*, pp. 1239-1260, 2007.

Song, X.D., R. Weaver, and X.N. Yang, Surface wave attenuation in Tibetan Plateau from ambient noise, Monitoring Research Review, Albuquerque, NM, 2012.

Stehly, L., M. Campillo, B. Froment, and R. L. Weaver, Reconstructing Green's function by correlation of the coda of the correlation (C^3) of ambient seismic noise, *J. Geophys. Res*., *113*, B11306, 2008.

Weaver R.L., On the amplitudes of correlations and the inference of attenuations, specific intensities and site factors from ambient noise, *C. R. Geoscience,* 343, pp. 615-622, doi:10.1016/j.crte.2011.07.001, 2011.

Weaver, R.L., On the retrieval of attenuation and site amplifications from ambient noise on linear arrays: further numerical simulations, *Geophys. J. Int.,* 193, 3, pp. 1644-1657, DOI: 10.1093/gji/ggt063, 2013.

Yang, X., S. R. Taylor, and H. J. Patton, The 20-s Rayleigh wave attenuation tomography for central and southeastern Asia, *J. Geophys. Res.,* 109, B12304, doi:10.1029/2004JB003193, 2004.

Zhang, J. and X.N. Yang, Extracting surface wave attenuation from seismic noise using correlation of the coda of correlation, J. *Geophys. Res.,* 118, pp. 1-15, doi:10.1002/jgrb.50186, 2013.

DISTRIBUTION LIST

DTIC/OCP 8725 John J. Kingman Rd, Suite 0944 Ft Belvoir, VA 22060-6218	1 cy
AFRL/RVIL Kirtland AFB, NM 87117-5776	2 cys
Official Record Copy AFRL/RVBYE/Dr. Robert Raistrick	1 cy